Lettuce Leaf Necrotic and Chlorotic Surface Defect Assessment Using Recurrent Neural Network Optimized by Electromagnetism-like Mechanism

Ronnie Concepcion II[*1] and Elmer Dadios[*2]

De La Salle University, Manila, Philippines
[*1]E-mail: ronnie_concepcionii@dlsu.edu.ph
[*2]E-mail: elmer.dadios@dlsu.edu.ph

Abstract. Detection of plant stress is crucial to improve cultivation management. This study presents a non-destructive solution in detecting lettuce crop health and quantitatively assessing the necrotic and chlorotic leaf surface defects due to drought-based senescence. A total of 210 matured lettuce images were collected over a week of water stressed testing using digital camera. Crop quality was classified into healthy and defective based on its canopy visual appearance using deep transfer image networks in which InceptionV3 bested other networks with accuracy of 97.321%. Necrotic and chlorotic regions of defective canopy were separately segmented using CIELab color space thresholding and extracted with color, texture, and morphological properties. Hybrid neighborhood component analysis and ReliefF confirmed that texture features are highly significant than colors for this problem. Artificial neurons on the three hidden layers of recurrent neural network (RNN) were fine-tuned using electromagnetism-like mechanism (EM). Combined EM-RNN exhibited the best R^2 performances of 0.9796 and 0.9565 in predicting necrotic and chlorotic surface defect percentages respectively. Necrosis has faster spread factor of 45.3419% than chlorosis in weekly basis per canopy. This developed comprehensive model of InceptionV3-EM-RNN is an objective, reliable and quantitative approach in providing quality assessment on leaf surface defect phenotyping.

Keywords: Computational Intelligence, Computer Vision, Crop Health Classification, Electromagnetism-like Mechanism, Leaf Quality Assessment

1. INTRODUCTION

Crop physical appearance, specifically the leaves, resembles the critical features that are easily affected by detrimental virus, bacteria and fungi, invading weeds, and abiotic factors such as thermal and water stresses [1-4]. It can be expressed visually through morphological, color and texture features. Flavor and aroma are subjectively evaluated unlike with visual appearance and biochemical compositions [5].

Plant senescence is the natural dying stage of plants that is normally characterized by leaves changing in colors and falling off from branch [6]. Aside from the fact that it is part of the crop life cycle by default, it can be triggered by environmental stresses such as abrupt change in ambient temperature, withdrawal from enough nutrient supply, and drought stress [7]. Thus, it can be classified as age-based senescence which comes into full maturity after the flowering life stage regulated by plant hormones and stress-based senescence that is activated by inducing inappropriate growth pre-harvest parameters on to the plant system. Senescence is widely observed through leaves as chlorophyll concentration is degraded transforming leaf tissue to yellowish in color known as chlorosis [8]. It is followed by necrosis which is the dying of leaf tissues characterized by brownish color [9]. Both chlorosis and necrosis are symptom indicators of distressed plants gradually resulting to senescence.

As senescence is visible and observable for farmers, this phenomenon can be indicators of agricultural malpractices. Traditionally, image processing is employed for faster visual inspection of crop leaf health and diseases. However, it significantly requires high resolution of images to accurately detect the defect. Computational intelligence is integrated with computer vision to yield better accuracy specially in understanding canopy related information in a bioregenerative advanced life support system (BALSS) [10] and technology-based greenhouses [11-12]. Lettuce canopy quality has been assessed using vision system based on red, green, blue (RGB), and hue, saturation, value (HSV) extracted color features of the defected area and artificial neural network (ANN) [5]. Support vector machine (SVM) using the third kernel polynomial was employed in classifying plant leaf diseases [13]. On the other hand, based on visual properties and crop reflectance of fresh cut lettuce, ammonia and arsenic levels of canopy surface was estimated [14-16]. Classifying crop quality is superficial in quantitatively understanding the intensity of defect on the canopy and computational analysis demands beyond this.

Detection of plant health and classifying it as healthy or unhealthy is not comprehensive enough in providing quantitative assessment on the quality of its canopy. With the abovementioned advancements in crop quality assessment, quantifying necrotic and chlorotic surface defect regions have not been done yet.

In this study, lettuce quality was classified into healthy and defective, and necrotic and chlorotic surface defect percentages were predicted using computer vision and computational intelligence (CI) models. 6-week matured lettuces were set to another week with suppressed water supply to activate drought-based senescence. Discoloration and drying on leaf tissues are the target spots to capture for assessing leaf quality. CI models were employed for both crop quality classification and senescence-induced leaf surface defect percentage prediction. The electromagnetism-like mechanism was chosen to optimize RNN as genetic algorithm and artificial bee colony resulted to global optimum convergence issue. The proposed model is a novel approach on quantitative assessment of necrotic and chlorotic regions using vision system. The developed model in this study is part of the 10-module vision-phenotype-lettuce (VIPHLET) model used for adaptive nutrient management in lettuce smart farm.

2. MATERIALS AND METHODS

Drought-induced senescence was quantitatively assessed by predicting necrotic and chlorotic covered surface percentages. The general architecture for developing the comprehensive crop health classification and necrotic and chlorotic surface defect region percentages prediction requires an RGB input image for feature engineering (Fig. 1). Matlab R2020a platform is the sole computational intelligence modeling software used in this study for image processing, feature extraction, feature selection, metaheuristic optimization, and surface defect percentage predictions.

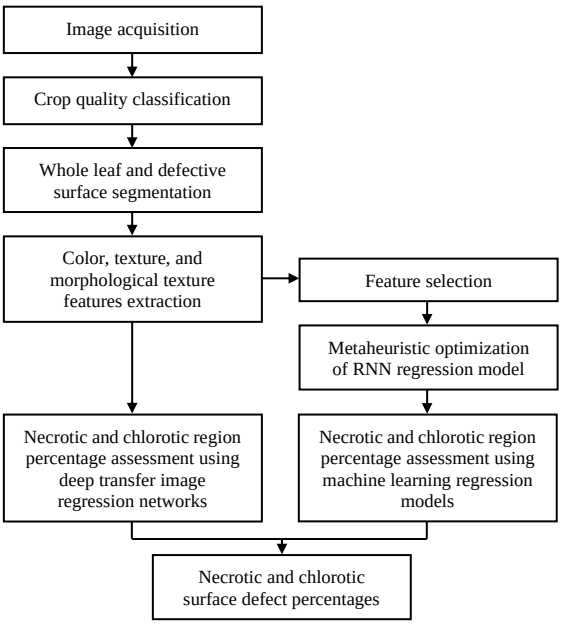

Fig. 1 General architecture of the construction of lettuce leaf necrotic and chlorotic surface damage assessment model

2.1. Phenotype Data Description and Experimental Condition

Loose-leaf lettuce is the chosen cultivar that was grown in a microclimatic closed environment aquaponic chamber in Morong, Rizal, Philippines with geographical coordinates of 14.5181° N and longitude of 121.2390° E. The aquaponic pond is filled with polyculture of tilapia and carps with maintained pH of 6 and electrical conductivity of 0.001 Siemens per centimeter. Nutrient film technique growth bed made of 3-inch food grade polyvinyl chloride pipes were employed inside the lettuce hydroponic chamber. The growth rack is equipped with artificial white lighting with 3,950 lumens using full spectrum T8 LED. Logitech IP camera was instrumentalized for the lettuce image acquisition vision system. The camera aspect ratio is 1:1 and the image spatial resolution is 3000 x 3000. There are 30 lettuces that were cultivated for 42-day full crop life cycle from germination to harvest stage. Another week was set for all crops with water supply suppressed. This was done to induce stress-based senescence through drought. No additional toxic chemicals were sprayed on the crops to stimulate discolorations. Without nutrients dissolved in water, lettuce leaf is subject to chlorosis due to incomplete crop growth factors. Chlorophyll will be inhibited due to lack of energy for circulation. It will be followed by drying of edges of the leaf which is necrosis. There is a total of 70 healthy matured lettuce images coming from 40 leaves and 30 whole canopies. Conversely, there is a total of 210 surface defective matured lettuces coming from 30 daily captured whole canopies in 7 days of drought.

2.2. Crop Quality Classification Modeling

Lettuce crop quality is canopy-based assessment by considering leaves with no brownish and yellowish spots as healthy lettuce and leaves with spots of discolorations as defective lettuce. Deep transfer image classification networks, namely MobileNetV2, ResNet101 and InceptionV3, were explored for this application. All these networks were configured using training optimizer of stochastic gradient descent with momentum (SGDM), minimum batch size of 10, maximum epochs of 6, initial learn rate of 0.0001, shuffle set to ‘every-epoch’, and validation frequency of 3. To avoid overfitting and improve training accuracy, image augmentation was employed using image reflection and translation over the pixel range of -30 to 30 in both horizontal and vertical axes. The deep transfer networks are evaluated based on accuracy, fall-out, precision, specificity, recall, F1-score, Matthew’s correlation coefficient, Hamming loss, and inference time.

2.3. Leaf Regions Segmentation

Among the possible color spaces, CIELab was utilized in image thresholding as manifested by its sensitivity to lightness and shadows considering that captured images are taken with the presence of photosynthetic light. It was technically chosen due to the fact that it is the scientific color spectrum and can be easily transformed from other spectrum without disrupting its quality [5]. The RGB input image was first converted into L*a*b* spectrum equivalent. For whole canopy segmentation from the non-vegetative background, L ranging from 1.113 to 99.371, a* of -26.016 to 31.076, and b* ranging of -3.583 to 79.304 were used. For necrotic regions segmentation from the non-vegetative background, L ranging from 42.547 to 99.71, a* of 1.434 to 37.197, and b* ranging of -1.061 to 58.778 were used. For chlorotic regions segmentation from the non-vegetative background, L ranging from 89.472 to 99.71, a* of -21.512 to 5.005, and

b* ranging of -1.061 to 58.778 were used. It can be noticed that for the defective surface regions, the b* component resembling the blue-yellow color axis is the same. More green colored pixels are eliminated for necrotic regions than chlorotic regions as denoted by a* component. Equally, lightness exhibited mostly by white pixels is significantly eliminated in segmenting necrotic regions as specified by L* component. It can be noticed that canopy edges exhibiting brownish color pixels are segmented and annotated to necrotic region with larger brown spots surfaces (Fig. 2). To further enhance the binarize images, image regions and holes were furtherly filled with white pixels.

2.4. Visible Feature Extraction

Three clusters of visible features were extracted in this study, namely color, texture and morphological. These features were considered as leaf necrosis and chlorosis are both characterized by discolorations, changes in surface roughness, and affected area. Color texture includes red, green, and blue component coming from the colored reflectance signals of the utilized IP camera. Texture feature includes the five properties of gray level co-occurrence matrix (GLCM) which are contrast, correlation, energy, entropy, and homogeneity. Morphological feature extracts the binary image area only as no other properties are needed for this study. Overall, each annotated image of necrotic and chlorotic regions contains this 8-feature vector.

2.5. Feature Selection

Hybrid neighborhood component analysis (NCA) and ReliefF feature selection models were employed on the original 8 visible features. Feature importance weights for NCA and ReliefF were ranked and averaged to determine the features with highest variance and impact to the system (Fig. 3.) NCA, is a supervised machine learning approach employing Mahalanobis distance in differentiating feature weights, selected correlation, entropy, and green component as the most impactful features. ReliefF, is a feature importance algorithm utilizing K-nearest neighbors to feature reduction, selected contrast, entropy, and homogeneity as the most relevant features to cause variations in output. With the combined results of NCA and ReliefF, contrast, entropy and homogeneity are the 3-feature vector with highest importance. These features will be used as predictors for predicting necrotic and chlorotic defect regions percentages.

2.6. RNN Model Parameters Tuning

Recurrent neural network (RNN) was configured using electromagnetism-like mechanism (EM) algorithm. EM is a physics-inspired optimization technique that uses the attraction and repulsion mechanism of charged particles in electromagnetic fields [17]. It was previously experienced that using genetic algorithm and particle swarm intelligence results to divergence issue, thus, it is rational to use electromagnetism-like mechanism as a potential approach that handles both constrained and unbounded problems [18].

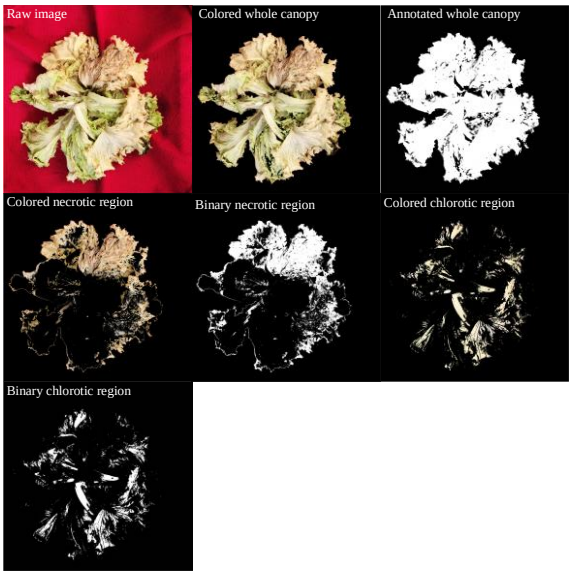

Fig. 2 Whole leaf and defective surface regions segmentation and binarization

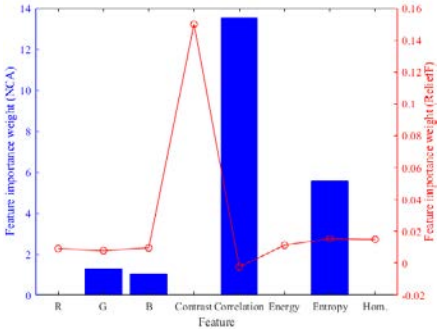

Fig. 3 Feature selection using neighborhood component analysis and RelifF

In this study, a linear regression equation was first derived using Minitab platform to symbolically model the relationship of number of neurons for first, second and third hidden layers (N_1, N_2, N_3) with the rendered model mean square error (MSE) where α of 0.001432 is bias, and β of 0.0000001, γ of 0.0000013, and δ of 0.000001 are the numerical coefficients for artificial hidden neurons (1). This MSE regression model serves as the objective function for EM where the attraction regions are defined. EM starts with initializing 50 particles in a 2-dimension hypercube in uniform distribution across [-200, -200] and [200, 200] lower and upper coordinate bounds. A particle is sampled from the electromagnetic space and calculated its objective function value. The particle with best objective function is set to x^{best}. It will then proceed with local search using delta value of 0.1 to determine the maximum feasible step length. If the coordinate determined by step length contains particle with better objective function value, then, current best particle is set to the new particle. This convergence approach is enabled by random line search algorithm. Technically, the objective function value is based on the particle charge of superposition principle where n is the number of particles, x is the particle at i and k coordinates, and m is the upper limit of coordinates (2). As particles are distributed on the electromagnetic space, it exhibits varying

intensity of charges that significantly affects the repulsion and attraction of the current best particle. The movement of this particle evaluated using total force vector exerted on each particle where j and m are the coordinate bounds and x and q are the particle displacement and charges at different coordinates (3). EM terminates and converges on global optimum after 500 iterations of neighborhood search per dimension in the electromagnetic hypercube without changes in the current best particle.

$$\mathrm{MSE} = \alpha - \beta N_1 - \gamma N_2 + \delta N_3 \quad (1)$$

$$q^i = exp\left(-n\frac{f(x^i)-f(x^{best}))}{\sum_{k=1}^{m} f(x^k)-f(x^{best})}\right) \quad (2)$$

$$F^i = \sum_{j\neq i}^{m}\left\{(x^j - x^i)\frac{q^i q^j}{\|x^j - x^i\|^2}\right\} \quad (3)$$

The hyperparameter tuning of RNN is configured by varying the number of particles distributed in the electromagnetic space used for initializing the preliminary space condition of system objective function (1), the dimension of electromagnetic hypercube, and maximum feasible step length that impacts the particle charge (2) and force vector (3). It can be realized that objective function value for 50 particles, electromagnetic hypercube dimension of 2 and maximum feasible step length of 0.01 yields the best particle charge function value. The optimal particle charge can be generated when the number of neurons in the first and second, and third layers are in the range of 100 to 150 and 20 to 80 respectively (Fig. 4).

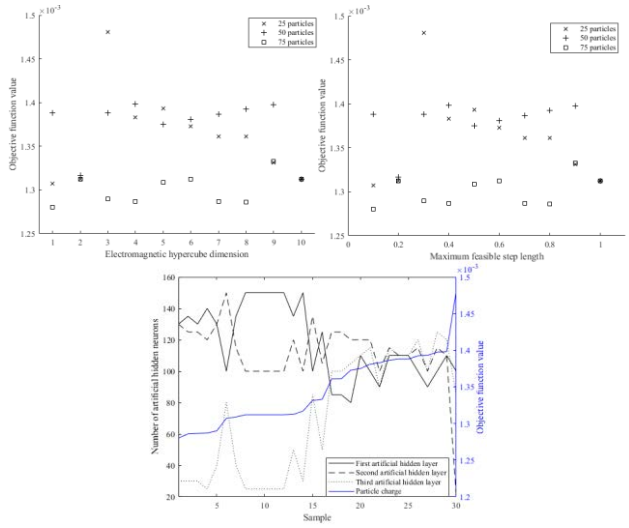

Fig. 4 Particle charge response with varying electromagnetic hypercube dimension and maximum feasible step length, and the interaction of artificial hidden neurons on RNN layers with particle charge

2.7. Feature-Based Machine Learning Regression for Surface Defect Percentage Prediction Modeling

Lettuce necrotic and chlorotic surface defect percentages were predicted using general processing regression (GPR), recurrent neural network and multigene symbolic regression genetic programming (MSRGP). GRP was optimized using sigma of 16.5101, beta of -2.323e4, squared exponential kernel function, exact predict method, and random active set method. RNN was optimized using electromagnetism-like mechanism resulting to 150, 100 and 50 artificial neurons configured on the first, second and third hidden layers. MSRGP was optimized using population size of 100, tournament size of 25 with activated lexicographic selection pressure, elite fraction of 0.7, pareto tournament probability of 0.7, maximum genes of 10, maximum tree depth of 5, ERC probability of 0.1, crossover rate of 0.84, mutation rate of 0.14, and expressional complexity measure function set of {'times', 'minus', 'plus', 'sqrt', 'square', 'sin', 'cos', 'exp', 'add3', 'mult3', 'tanh', 'log', 'cube', 'negexp', 'neg', 'abs'}. The input set to these machine learning regression models are the numerical feature vectors of contrast, entropy, and homogeneity. To differentiate the impact of NCA-RelifF feature selection, the default 8-feature vector was also set as input for exploration.

2.8. Deep Transfer Image Regression for Surface Defect Percentage Prediction Modeling

Aside from feature-based machine learning models, deep transfer image regression networks of MobileNetV2, ResNet101 and InceptionV3 were explored to predict necrotic and chlorotic defective regions separately. These networks were configured using training optimizer of stochastic gradient descent with momentum (SGDM), minimum batch size of 20, maximum epochs of 7, initial learn rate of 0.0001, learn rate schedule set to piecewise, learn rate drop factor of 0.1, learn rate drop period of 20, shuffle set to 'every-epoch', and validation frequency of 3. To avoid overfitting and improve training accuracy, image augmentation was employed using image reflection and translation over the pixel range of -30 to 30 in both horizontal and vertical axes. The input set to these transfer networks are the raw lettuce images as deep learning models have mathematical relations selection model on its hidden layers using convolutional neural network (CNN). In this way, the configured MobileNetV2, Resnet101 and InceptionV3 models are tested for real time evaluation of acquired images. Root mean square error (RMSE), R^2, and mean absolute error (MAE) are used as evaluation metrics.

3. Results and Discussions

3.1. Crop Quality Classification

Matured lettuce canopies were classified healthy and defective using MobileNetV2, ResNet101 and InceptionV3. From the 42 test images, 14 are tagged as healthy and 28 are defective lettuces with samples shown in Fig. 5. Healthy crops are those lettuces that were captured during the seventh week of crop life cycle with standard water supply. In Fig. 5, one-hot data encoding is employed which defines 1 as healthy lettuce and 0 as defective lettuce. It was arranged in order that samples 1 to 28 are the defective lettuces and the remaining samples are the healthy lettuces. MobileNetV2 failed to correctly classify two defective lettuces. ResNet101 and InceptionV3 have same accuracy of 97.321% due to one misclassification (Table 1). However, InceptionV3 bested ResNet101 based on their inference time with 1038 seconds for InceptionV3 and 1659 seconds on the latter. This made InceptionV3 the most considerable crop quality classification model to be tandem with the drought-based senescence-induced surface defect percentages prediction model.

3.2. Surface Defect Percentage Prediction Using Feature-Based Machine Learning Regression

Defective matured lettuces with drought-based senescence that exhibit necrosis and chlorosis on its canopy surface were quantitatively assessed by predicting the affected regions using optimized GPR, RNN and MSRGP. In Fig. 6, machine learning models were suffixed with numerical subscripts of 8 and 3 denoting the number of predictors used such as RNN_8 for RNN using 8 predictors. 8-feature vector utilizes the complete color and texture features while 3-feature utilizes the NCA-ReliefF selected features. For both necrotic and chlorotic surface defect percentages predictions, EM-optimized RNN_3 performed the best estimations with R2 of 0.9796 and 0.9565 respectively (Table 2). GRP_3 exhibited the lowest necrotic region percentage prediction accuracy with R^2 of 0.8396, however, it can be noticed that $MSRGP_3$ has R^2 of 0.9132 but very erroneous predictions characterized by its RMSE of 2833734.76. Similarly, $MSRGP_3$ rendered the poorest performance in predicting chlorotic region percentage among other feature-based machine learning models with RMSE of 4264.4682 as to compare with 4.7258 RMSE of EM-optimized RNN_3 (Table 2). The relative error of EM-RNN in predicting necrotic region significantly diminished in a measure of 22.2826% by using the 3 selected predictors instead of 8, thus, prediction accuracy increased by 0.6384%. Correspondingly in predicting the chlorotic region percentage, using RNN_3 instead of RNN_8 drastically diminished the RMSE to 67.4156% from 6.3652 and a 46.419% increase in accuracy. As requirement for low-computational cost intelligent system, RNN_3 also yielded the shortest inference time with 4 seconds in predicting necrotic percentage and 2 seconds in for chlorotic percentage. Evidently, the use of contrast, energy, and homogeneity as the only predictors for EM-RNN significantly improved its performance making it the most sensitive and reliable feature-based machine learning model for this application.

3.3. Surface Defect Percentage Prediction Using Deep Transfer Image Regression

In contrast from GPR, RNN and MSRGP, MobileNetV2, ResNet101 and InceptionV3 utilized no features instead raw images of lettuce such as the defect image shown in Fig. 5. For necrotic region percentage, InceptionV3 performed the best prediction R^2 of 0.8789 among other deep transfer networks (Fig. 7). However, MobileNetV2 has 40% faster inference time compare to InceptionV3. For chlorotic region percentage, MobileNetV2 exhibited the best prediction R^2 of 0.8641 while ResNet101 has the shortest inference time of 647 seconds (Table 2).

3.4. Synthesis

After successful multifold explorations in predicting the percentages of affected lettuce canopy regions due to drought-induced senescence using feature-based machine learning models and deep transfer image networks, it can be deduced that EM-RNN_3 exhibited the most accurate and sensitive model amongst GRP, MSRGP, MobileNetV2, ResNet101 and InceptionV3. Exactness and inference-wise, EM-RNN_3 provided results that can be implemented for comprehensive computational lettuce phenotyping. Despite of the model complexity and built-in evolutionary-based optimizer of MSRGP it still rendered the poorest results for feature-based models. The seamless model of integrated crop quality classification and senescence affected regions percentages prediction of InceptionV3-EM-RNN resulted to more quantitative understandings of the scope of water stress impact to lettuce unlike a mere classifying if the crop is healthy or damaged [5]. The result of this vision-based model can also be used in quantifying the spots incurred on leaf surfaces for post-harvest lettuce [2].

It was also realized that despite of the discolorations as visual basis of crop enthusiasts to deduce that a crop is undergoing senescence, the developed NCA-ReliefF proved that texture features reveal more accuracy on it. Moreover, necrosis increased by 1.2857% daily and 45.3419% after 7 days for a whole lettuce canopy. Lettuce chlorosis increased by 11.1406% daily and 26.5704% over a week period. Overall, necrosis has faster spread rate compare to chlorosis making the edge of the leaves to turn dry and lose all chlorophyll avoiding extension of photosynthesis.

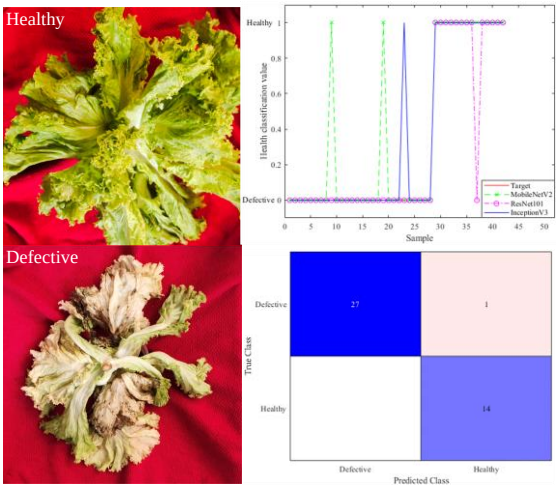

Fig. 5 Samples of healthy and defective matured lettuces, comparison of target and deep transfer image networks crop quality classification outputs, and confusion matrix of InceptionV3

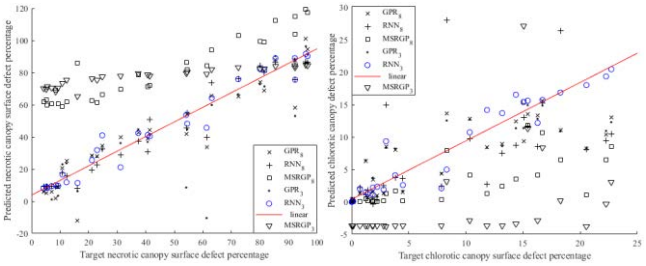

Fig. 6 Regression curves for feature-based machine learning regression approach of predicting necrotic and chlorotic surface defect percentages

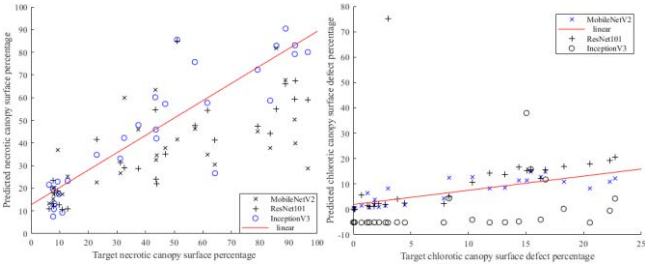

Fig. 7 Regression curves for deep transfer image regression approach of predicting necrotic and chlorotic surface defect percentages

Table 1. Evaluation of Lettuce Crop Quality Classification Using Deep Transfer Image Networks

Model	Training	Validation	Testing								
	Accuracy	*Accuracy*	*Accuracy*	*Fall-out*	*Precision*	*Specificity*	*Recall*	*F1-score*	*MCC*	*Hamming Loss*	*Inference Time (s)*
MobileNetV2	92.860	95.240	0.946	0.033	0.964	0.967	0.938	0.948	0.907	0.049	965
ResNet101	92.860	97.620	0.973	0.033	0.964	0.967	0.983	0.973	0.949	0.026	1659
InceptionV3	95.240	97.620	0.973	0.017	0.982	0.983	0.967	0.974	0.950	0.026	1038

Table 2. Evaluation of Lettuce Necrotic and Chlorotic Surface Defect Percentages Prediction Using Computational Intelligence Regression Models

Model	Training			Validation			Testing			
	RMSE	R^2	*MAE*	*RMSE*	R^2	*MAE*	*RMSE*	R^2	*MAE*	*Inference Time (s)*
Necrotic Region Percentage Prediction										
GPR	23.431	0.549	20.610	6.316	0.972	4.660	17.262	0.840	9.039	18.204
RNN	5.080	0.983	3.986	4.301	0.987	3.169	6.164	0.980	4.095	4.000
MSRGP	3.314E+06	0.919	3.308E+06	3.078E+06	0.958	2.834E+06	3.073E+06	0.913	2.824E+06	5.340
MobileNetV2	11.251	0.598	42.365	18.039	0.652	8.745	24.850	0.616	20.130	240
ResNet101	19.900	0.747	35.745	9.509	0.784	7.144	20.911	0.772	16.872	929
InceptionV3	14.110	0.870	22.748	10.216	0.887	4.112	14.448	0.879	10.845	600
Chlorotic Region Percentage Prediction										
GPR	3.021	0.868	2.032	2.262	0.885	1.529	4.411	0.818	2.964	14.787
RNN	7.688	0.418	5.118	6.843	0.386	4.726	2.074	0.957	1.260	2
MSRGP	3.042E+03	0.549	2.684E+03	2.837E+03	0.642	2.239E+03	4.264E+03	0.428	2.742E+03	5.040
MobileNetV2	11.251	0.741	2.477	18.039	0.914	1.965	3.546	0.864	2.801	875
ResNet101	19.900	0.196	8.336	9.509	0.325	5.788	20.096	0.185	6.394	647
InceptionV3	14.110	0.688	3208.887	10.216	0.633	2874.635	5931.297	0.570	3850.812	668

4. CONCLUSION AND RECOMMENDATION

Lettuce quality based on canopy features was classified into healthy and defective using InceptionV3. Drought-based senescence-induced necrosis and chlorosis were observed using NCA-ReliefF selected contrast, entropy, and homogeneity features making texture features highly significant than color features. EM-RNN bested other feature-based machine learning and deep transfer image models in predicting necrotic and chlorotic surface defect percentages separately. Necrosis has faster spread factor compare to chlorosis for matured aquaponic lettuce that undergoes suppressed water supply. The developed InceptionV3-EM-RNN model is highly useful for computational lettuce phenotyping. For future studies, it is recommended to use this model approach in monitoring post-harvest lettuce quality for proper storage.

Acknowledgments

The authors would like to acknowledge the support of the Engineering Research and Development for Technology (ERDT) of the Department of Science and Technology (DOST) of the Philippines and the Intelligent Systems Laboratory of the De La Salle University, Philippines.

REFERENCES:

[1] L. Hadad, N. Luria, E. Smith, N. Sela, O. Lachman, and A. Dombrovsky, "Lettuce chlorosis virus disease: A new threat to cannabis production," Viruses, vol. 11, no. 9, pp. 1–14, 2019.

[2] P. Kongwong, D. Boonyakiat, and P. Poonlarp, "Extending the shelf life and qualities of baby cos lettuce using commercial precooling systems," Postharvest Biol. Technol., vol. 150, no. September 2018, pp. 60–70, 2019.

[3] N. D. Adhikari, I. Simko, and B. Mou, "Phenomic and physiological analysis of salinity effects on lettuce," Sensors (Switzerland), vol. 19, no. 21, 2019.

[4] W. Zorrig, A. El Khouni, T. Ghnaya, J. C. Davidian, C. Abdelly, and P. Berthomieu, "Lettuce (Lactuca sativa): A species with a high capacity for cadmium (Cd) accumulation and growth stimulation in the presence of low Cd concentrations," J. Hortic. Sci. Biotechnol., vol. 88, no. 6, pp. 783–789, 2013.

[5] I. C. Valenzuela et al., "Quality assessment of lettuce using artificial neural network," HNICEM 2017 - 9th Int. Conf. Humanoid, Nanotechnology, Inf. Technol. Commun. Control. Environ. Manag., August 2018, pp. 1–5, 2018.

[6] J. Ripoll et al., "Transcriptomic view of detached lettuce leaves during storage: A crosstalk between wounding, dehydration and senescence," Postharvest Biol. Technol., vol. 152, no. February, pp. 73–88, 2019.

[7] L. L. Petrazzini, G. A. Souza, C. L. Rodas, E. B. Emrich, J. G. Carvalho, and R. J. Souza, "Nutritional deficiency in crisphead lettuce grown in hydroponics," Hortic. Bras., vol. 32, no. 3, pp. 310–313, 2014.

[8] S. G. Kunjeti et al., "Detection and quantification of Bremia lactucae by spore trapping and quantitative PCR," Phytopathology, vol. 106, no. 11, pp. 1426–1437, 2016.

[9] K. Kubota and J. C. K. Ng, "Lettuce chlorosis virus P23 suppresses RNA silencing and induces local necrosis with increased severity at raised temperatures," Phytopathology, vol. 106, no. 6, pp. 653–662, 2016.

[10] A. C. Schuerger, K. L. Copenhaver, D. Lewis, R. Kincaid, and G. May, "Canopy structure and imaging geometry may create unique problems during spectral reflectance measurements of crop canopies in bioregenerative advanced life support systems," Int. J. Astrobiol., vol. 6, no. 2, pp. 109–121, 2007.

[11] T. Chokey and S. Jain, "Quality Assessment of Crops using Machine Learning Techniques," Proc. - 2019 Amity Int. Conf. Artif. Intell. AICAI 2019, pp. 259–263, 2019.

[12] A. Rahman and B. K. Cho, "Assessment of seed quality using non-destructive measurement techniques: A review," Seed Sci. Res., vol. 26, no. 4, pp. 285–305, 2016.

[13] K. M. Chaitra, F. Anjum, I. P. Harshitha, D. M. Meghana, and M. V Rachitha, "Plant Leaf Disease Identification System for Android," Ijercse, vol. 5, no. 6, pp. 48–53, 2018.

[14] B. Pace, M. Cefola, P. Da Pelo, F. Renna, and G. Attolico, "Non-destructive evaluation of quality and ammonia content in whole and fresh-cut lettuce by computer vision system," Food Res. Int., vol. 64, pp. 647–655, 2014.

[15] F. S. Farnese, J. A. Oliveira, F. S. Lima, G. A. Leão, G. S. Gusman, and L. C. Silva, "Avaliação do potencial de Pistia stratiotes L. (alface d'água) para a bioindicação e fitorremediação de ambientes aquáticos contaminados com arsênio," Brazilian J. Biol., vol. 74, no. 3, pp. 103–112, 2014.

[16] N. Katsoulas, A. Elvanidi, K. P. Ferentinos, M. Kacira, T. Bartzanas, and C. Kittas, "Crop reflectance monitoring as a tool for water stress detection in greenhouses: A review," *Biosyst. Eng.*, vol. 151, pp. 374–398, 2016.

[17] S. Birbil, and S. Fang, "An electromagnetism-like mechanism for global optimization," Journal of Global Optimization, vol. 25, no. 3, pp. 263-283, 2003.

[18] Q. Wu, W. Xu, and W. Huang, "Applications of an improved electromagnetism-like mechanism algorithm in optimization of processing parameters," ACM International Conference Proceeding Series, pp. 320-325, 2018.